Journal of Physiology (2002), **545.2**, *pp.* 509–520
DOI: 10.1113/jphysiol.2002.022095

www.jphysiol.org

Properties of mEPSCs recorded in layer II neurones of rat barrel cortex

Christopher R. L. Simkus and Christian Stricker

Institute of Neuroinformatics, University of Zürich and Federal Institute of Technology (ETH), Winterthurerstrasse 190, CH-8057 Zürich, Switzerland

Voltage-clamp recordings from layer II neurones in somatosensory cortex of rats aged between 12 and 17 days showed a high frequency of spontaneous postsynaptic currents (sPSCs), which on average was 33 ± 13 Hz (S.D.). sPSCs were mediated largely by glutamatergic AMPA receptors. Their rates and amplitudes were independent of blocking sodium channels with 1 μM tetrodotoxin (TTX). Most of them, therefore, represent genuine miniature excitatory postsynaptic currents (mEPSCs). The rise time of the fastest (10 %) mEPSCs was 288 ± 86 μs (10–90 %) and the half-width was 1073 ± 532 μs. The amplitude was −5.9 ± 1.1 pA with a coefficient of variation (CV) of 0.44 ± 0.14. The rate of mEPSCs was very temperature sensitive with a Q_{10} (33–37 °C) of 8.9 ± 0.9. Due to this temperature sensitivity, we estimated that the microscope lamp contributed an increase in temperature of about 4 °C to the tissue in the focal volume of the condenser. Cell-type differences in the rate of mEPSCs were found between pyramidal/multipolar and bipolar cells. The latter had a frequency of about a third of that seen in the other cell groups. Recordings in layer II are ideally suited to investigate mechanisms of spontaneous transmitter release.

(Received 8 April 2002; accepted after revision 23 September 2002; first published online 11 October 2002)
Corresponding author C. Stricker: Institute of Neuroinformatics, University of Zürich and Federal Institute of Technology (ETH), Winterthurerstrasse 190, CH-8057 Zürich, Switzerland. Email: christian.stricker@ini.phys.ethz.ch

Since neocortical neurones receive approximately 10 000 synaptic inputs (Larkman, 1991) and each neurone fires spontaneous action potentials at a rate of 0–5 Hz (Gilbert, 1976), neurones in cortical areas would be expected to receive a continuous barrage (⩽ 50 kHz) of spontaneous postsynaptic potentials (sPSPs) *in vivo*. However, after focal application of TTX to cat neocortical tissue *in vivo*, a sPSP rate of around 21 Hz was observed (Paré *et al.* 1997). Under *in vitro* conditions, it is very rare to observe sPSP frequencies that exceed 20 Hz. A good example of this is the rat hippocampal slice, which shows an average frequency of 1–2 Hz (Manabe *et al.* 1992).

In layer II of rodent somatosensory cortex, neurones receive over 70 % of their synaptic inputs from neurones nearby (Gruner *et al.* 1974). We wondered if under these conditions a high rate of sPSCs could be observed and if these were indeed due to spontaneous action potentials. We therefore characterised the basic features of spontaneous transmitter release. It serves as the basis for the subsequent paper (Simkus & Stricker, 2002), in which we test the hypothesis that spontaneous transmitter release is the result of calcium (Ca^{2+}) release from intracellular Ca^{2+} stores.

METHODS

Slice preparation and whole-cell recording

Twelve- to seventeen-day-old Wistar rats were decapitated with a guillotine and the brain rapidly removed and placed into ice-cold artificial cerebrospinal fluid (ACSF) containing (mM): NaCl, 125; KCl, 2.5; $NaHCO_3$, 25; NaH_2PO_4, 1.25; $CaCl_2$, 2; $MgCl_2$, 1; glucose, 10; gassed with 95 % O_2 and 5 % CO_2 (Oxycarbon), to obtain a final pH of 7.4. The osmolarity was 315 mosmol l^{-1}. The brain was then hemisected along the midline and the cut surfaces glued onto the stage of a vibratome (TPI, Series 1000, St Louis, MO, USA), with cyanoacrylic glue (Loctite 406). The stage was set at a forward tilting angle of 15 deg. The vibratome chamber was filled with ice-cold, gassed ACSF, and slices were cut to a thickness of 300 μm. The slices of cortex with the hippocampus attached were placed in a holding chamber containing gassed ACSF for 1 h at 35 °C and maintained later at room temperature (22–24 °C) until used in experiments. The methods were approved by the veterinary office of the Canton of Zürich and conform to Swiss Federal legislation.

Whole-cell recordings were made from neurones in upper layer II of rat somatosensory cortex using patch electrodes (tip resistance 3–4 MΩ), pulled from thick-walled borosilicate glass (o.d. 2 mm, i.d. 1 mm, Hilgenberg, Oberkochenhofen, Germany), using a Brown-Flaming type horizontal puller (P97, Sutter Instruments, Novato, CA, USA). The intracellular solution contained (mM): gluconic acid, 115; KCl, 20; HEPES, 10; phosphocreatine, 10; ATP-Mg, 4; Na-GTP, 0.3; biocytin, 0.5 %; pH titrated to 7.3 (1 M KOH), osmolarity 305 mosmol l^{-1}. All experiments were conducted at 33 ± 1 °C, with the IR lamp on (nominally 37 °C) and with an increased glucose concentration (25 mM) in the ACSF (330 mosmol l^{-1}).

Whole-cell recordings were obtained under visual control as described in Stuart *et al.* (1993) on an Axioskop 2F microscope (Zeiss, Oberkofen, Germany) using a × 40 long-working distance lens (NA 0.8) and with the infra-red filter between the light source and the condenser removed. sPSCs were recorded in continuous

voltage-clamp at a holding potential of −70 mV or in current-clamp with an Axopatch 200B amplifier (Axon Instruments, Union City, CA, USA). The signals were filtered at 2 kHz (8-pole Bessel), the holding current subtracted using a sample-and-hold (design JCSMR, ANU, Canberra, Australia) and digitised at 5 kHz using an ITC-18 computer interface (Instrutech Corporation, Port Washington, NY, USA). Data were acquired using in-house software developed for IGOR Pro 4.0 (Wavemetrics, Lake Oswego, OR, USA) on a Macintosh PowerPC.

Series resistance (R_s), electrode and whole-cell capacitance were not compensated, nor were the voltage values corrected for junction potential (7 mV). R_s and input resistance (R_{in}) were monitored between each sPSC recording by applying a brief depolarising voltage step (0.5 mV) and measuring the resulting current response. R_s was estimated from the peak amplitude of the capacitive transient using Ohm's law and R_{in} as the difference between R_s and the total resistance, calculated from the steady state current. Experiments were discarded if either R_s or R_{in} changed by more than 15 %. The negative sign of inward currents has been omitted in the text to indicate magnitude.

To assess the excitability of the neurones and to block voltage-dependent calcium channels (VDCCs) with divalent cations, ACSFs of different compositions were used. The aim was to maintain, where possible, iso-osmotically the same Ca^{2+} or divalent cation concentration to prevent disruption of surface charges by a compensatory change in NaCl. The low excitability solutions (LES) contained either 1 or 0.1 mM KCl. For the high Mg^{2+} solution, NaCl was reduced to 118 mM and $MgCl_2$ increased to 6 mM. For solutions containing either 0.1 mM Cd^{2+} or Ni^{2+}, NaCl was 126.25 mM and NaH_2PO_4 was omitted to avoid precipitation of insoluble phosphates.

All drugs were purchased from Sigma (Buchs, Switzerland) except tetrodotoxin (TTX, Latoxan, Rosans, France) and 2,3-dioxo-6-nitro-1,2,3,4-tetrahydrobenzo[f]quinoxaline-7-sulphonamide (NBQX, Tocris Cookson, Bristol, UK). TTX, bicuculline, glutamine, kynurenic acid, and NBQX were all prepared as stock solutions and added to the superfusate later.

Data analysis

Recordings were analysed offline for sPSCs using a detection plug-in for Axograph 4.6 (Axon Instruments). This program makes use of a scaling-template method (Clements & Bekkers, 1997), in which a representative time course of a sPSC is used to calculate a detection criterion by optimally scaling parameters in amplitude and time. A spontaneous event was considered representative if neither the baseline, rise time nor decay time straddled another sPSC, if the noise on the time course was symmetrical and if it matched the average sPSC time course as determined by eye.

To allow the detection of all PSC shapes by the program, a low threshold was chosen. However, this resulted in the detection of events which were not different from recording noise. This required a second criterion, which corresponded to 2.5 times the noise standard deviation of recording sequences without sPSCs identified manually. For each analysis, the template and second threshold level were interactively optimised until the result closely matched the number of sPSCs identified by eye. The first 2 s of every recording was analysed manually and typically contained around 50 to over 100 sPSCs. Figure 1*A* shows an example in which, based on the template illustrated in Fig. 1*B*, the program recovered 65 of 67 events identified by eye. The template chosen consisted of a short baseline period (⩽ 1 ms), a complete rising but only a partial (~50 %) decay phase of the current. The latter was subject to the interactive optimisation.

A high frequency of sPSCs implies that collisions (at least two events with overlapping time courses) are very common. Most sPSCs with overlapping time courses could be detected provided the decay phase of the event was longer than that of the template. Practically, we were unable to reliably detect sPSCs with intervals shorter than 1.2 ms. Based on an optimal template choice, we were able to detect > 95 % of the events identified by eye.

Comparison of cumulative probability density functions was performed using Kolmogorov-Smirnov statistics (P_{KS}). Average values were compared using *t* tests (P_t) or paired *t* tests (P_{pt}). The significance of linear correlations was based on Pearson's *r* (P_r). The level of significance was $P < 0.05$. Values are given as means ± S.D.

Recording temperature

The temperature of the ACSF in the recording chamber was controlled by a water jacket at the inlet to the chamber and monitored using a thermocouple attached to a multimeter, which had been calibrated with a regular mercury thermometer. To account for the heat generated by the microscope lamp, the thermocouple was positioned as close as possible to the tip of the recording electrode. Temperature changes in the recording chamber of a few degrees could be obtained within 2–4 min.

The temperature dependence of sPSC frequency was expressed as Q_{10}, which was calculated with the following equation (Johnson *et al.* 1954):

$$Q_{10} = \left(\frac{X_2}{X_1}\right)^{10/(T_2-T_1)},$$

where T_1 corresponds to the lower and T_2 to the higher temperature in absolute temperature units (kelvins), and X_1 and X_2 are the frequencies at the corresponding temperatures. The fitting procedure used (available in IGOR 4.0) is based on a chi-squared argument (Levenberg-Marquardt) and returns error estimates of the parameters.

Histology and cell identification

Biocytin at 0.5 % was routinely included in the intracellular solution. Following the recording, the electrode was gently retracted from the cell and the slice was fixed in a 0.1 M phosphate buffer solution containing 4 % paraformaldehyde and stored in the refrigerator until further processing. The details are given in Kawaguchi *et al.* (1989) and are based on Horikawa & Armstrong (1988).

Neurones in layer II were chosen on the basis of IR-DIC images and classified based on a microscopic evaluation of the histological specimens. The following definitions according to Keller (1995) were used to classify the different cell types. A pyramidal cell has a large pyramidal-shaped soma with a primary apical dendrite and basal dendrites; a multipolar cell is a non-pyramidal cell with up to 10 primary dendrites radiating in all directions from the soma; and a bipolar cell has a spindle-like soma with dendritic trunks arising preferentially from the apical and basal poles of the soma.

To insure recordings from a homogeneous population of cells, all recordings were from pyramidal/multipolar cells, unless stated otherwise.

RESULTS

Recording mode: voltage- *versus* current-clamp

Preliminary experiments showed a high rate of sPSCs of up to 50–100 Hz. We therefore required a recording mode, which could optimally follow the rates of release. Since in current-clamp the decay of the sPSC is shaped by the time constant of the cell, we expected that voltage-clamp conditions, though not perfect (space-clamp problems), might be favourable. Voltage- and current-clamp recordings were made from the same layer II neurone at $V_h = -70$ mV or at resting membrane potential, which was –67 mV. An example with a low frequency of synaptic events was chosen to minimise overlaps between sPSCs or sPSPs, and, therefore, enable good temporal resolution. Figure 1*C* and *D* shows the first 2 s of this 10 min recording in voltage- and current-clamp, with an average frequency of 12.5 ± 0.6 and 11.6 ± 1.0 Hz, respectively. The current-clamp recording was filtered at 1 kHz due to the slower kinetics of the PSPs. Figure 1*E* shows representative synaptic events (not averaged) used as templates to detect the spontaneous events in the two recording modes. The voltage-clamp template (black) covered 3.8 ms, and the one for current-clamp (grey) 16.6 ms. The two results for the frequencies differed significantly from each other ($P_{KS} \ll 0.001$), as illustrated in Fig. 1*F* with the average instantaneous frequencies (f_1) 38.1 ± 59.4 and 23.3 ± 25.1 Hz, respectively. This indicates that significantly more spontaneous events can be recovered in voltage- than in current-clamp.

It is possible to conservatively estimate the approximate number of detection errors that would occur in a given

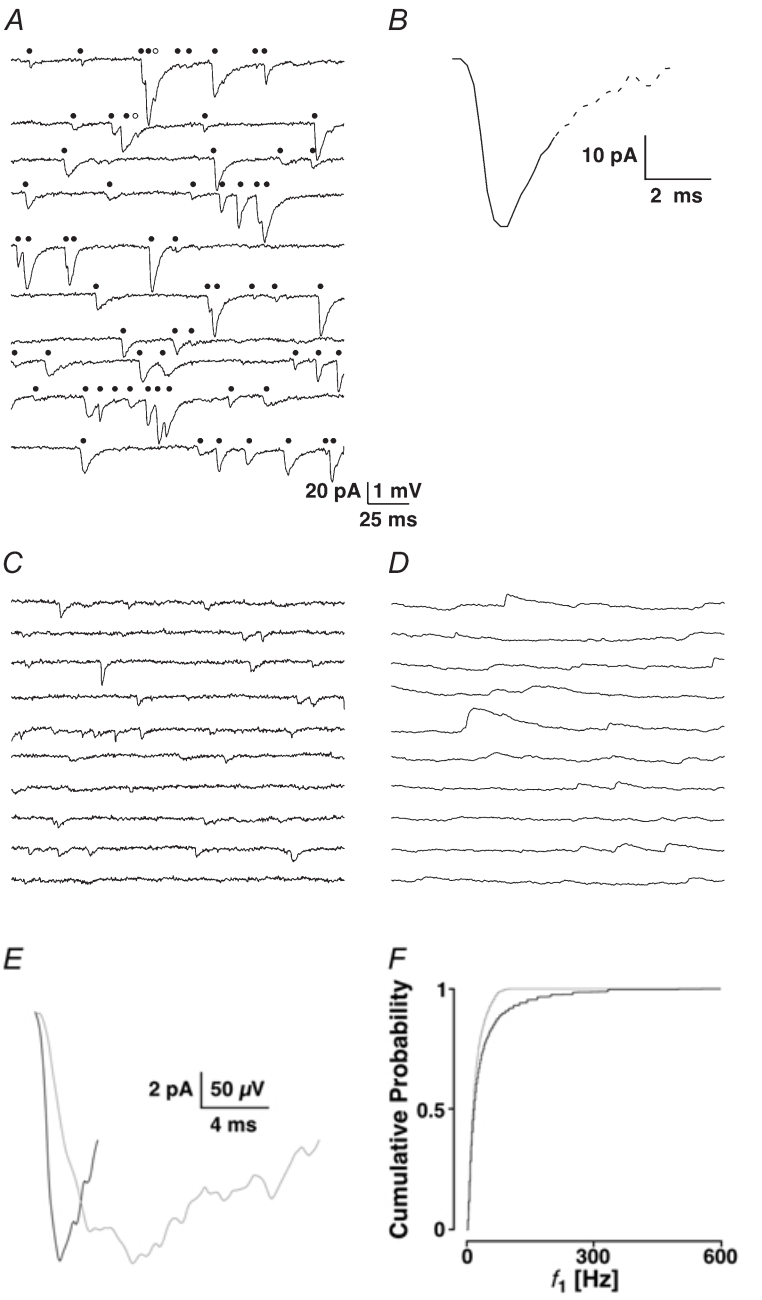

Figure 1. Manual and algorithmic identification of sPSCs, choice of the template and recording mode

A, the first 2 s of a recording epoch broken up into 200 ms periods, each vertically separated. The total number of events detected by eye was 67, of which 65 were recovered (●) and two were considered as missed (○) by the template-matching algorithm. *B*, the template was chosen from a representative PSC. The template is truncated (continuous line), with the truncated portion of the time course indicated by the dashed line. *C* and *D*, two subsequent recording sequences from the same cell illustrated in voltage- and current-clamp, respectively. *E*, the two templates used to detect spontaneous synaptic currents in voltage- (black) and current-clamp (grey). The current-clamp template has been inverted to allow for better comparison. *F*, cumulative probability density functions (cPDF) of f_1 for the data recovered in voltage- and current-clamp shown in black and grey, respectively.

recording, assuming that the duration of the template approximates the ability to detect events using the formula $P(t \leqslant \Delta t) = 1 - \exp(-\lambda \Delta t)$, where λ represents the average rate and Δt is the length of the template. In reality, Δt could be smaller than the time course of the template. In our example and at an average frequency of 10 Hz, approximately 3.5 % of sPSCs overlap when recorded in voltage-clamp. In current-clamp, the proportion is about 20 %. This difference becomes even more critical at higher frequencies, where, for example at 60 Hz, 73 % of the events recorded in current-clamp will be found to collide within the time window of the template. This contrasts with 19.4 % in voltage clamp. These considerations convinced us to perform all subsequent recordings in voltage-clamp.

Properties of sPSCs and mPSCs

A typical recording sequence is illustrated in Fig. 2*A*. As with all recordings, this example was first assessed for stationarity by inspection of the plots shown in Fig. 2*B*. Since both amplitudes and frequency were considered stationary (not shifting more than ± 10 % around the average value during half a minute), this experiment was considered acceptable for a full analysis. Over the 610 s of recording, 25 159 sPSCs were detected, resulting in an average frequency of 41 ± 2 Hz, and average peak amplitude of 10.3 ± 8.9 pA. f_1 had an average value of 85 ± 82 Hz. Typically, the histograms of f_1 and amplitudes had a prominent peak at ~30 Hz and ~4.5 pA, respectively, followed by a pronounced tail (Fig. 2*C* and *D*). Cumulative probability density functions (cPDFs) were formed by integrating and normalising the histograms of f_1 and amplitudes (Fig. 2*E* and *F*).

In this example, the average sPSC time course had a slow rising and decay phase. This slow time course is due to averaging of all events from different electrotonic locations on the dendritic tree with poor voltage-clamp and sPSCs involved in collisions (kinetic data of a subset of currents is given below). On the basis of eight recordings, the sPSC had a frequency of 33 ± 13 Hz, a peak amplitude of 9.9 ± 2.7 pA, an average rise time (10–90 %) of 0.7 ± 0.8 ms, and an average half-width of 2.1 ± 3.8 ms.

We were concerned because the rate of sPSCs observed was significantly higher in our preparation than that reported for other preparations (range: 5–20 Hz). To check if the rate observed was due to some preparational/recording

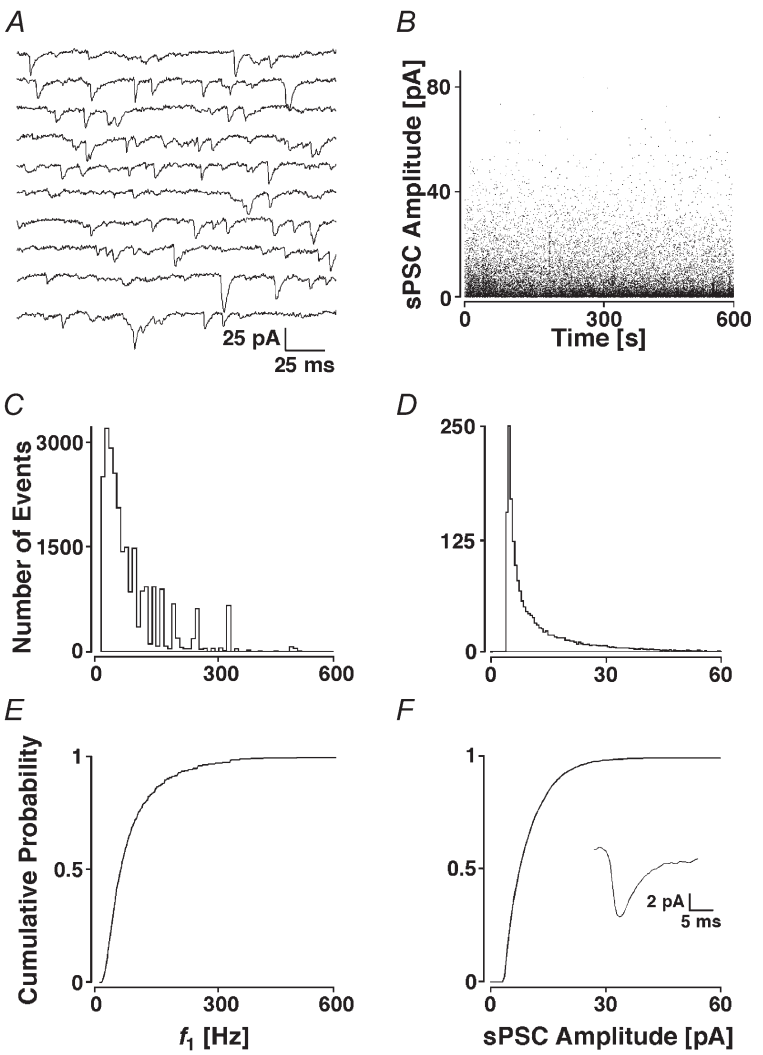

Figure 2. sPSCs from a layer II pyramidal neurone

A, recording epoch of 2 s. *B*, individual sPSC amplitudes plotted against the time during the recording. Note the stationarity of the process. *C*, histogram of f_1 sorted into bins of 10 Hz and *D*, peak amplitudes assigned to bins of 0.5 pA. *E* and *F*, cPDFs of the histograms shown in *C* and *D* with the average sPSC time course from the first 100 events illustrated in the inset.

artefact, or reflected a physiological feature of the layer II terminals, we recorded in sequence in the same slice from a layer II neocortical and later from a hippocampal CA1 pyramidal cell as an internal reference. Such an experiment is shown in Fig. 3, with a recording from a layer II and a CA1 pyramidal cell in *A* and *B*, respectively. The average sPSC frequencies were 58 ± 3 and 2.0 ± 0.1 Hz, respectively. There was a significant difference in the distributions of f_1 (Fig. 3*C*), the mean value of which was 107 ± 96 Hz for the layer II and 8 ± 13 Hz for the CA1 neurone ($P_{KS} \ll 0.001$). The sPSCs showed an average amplitude of 7.7 ± 4.7 (layer II) and 7.3 ± 7.0 pA (CA1), which were not significantly different ($P_{KS} = 0.3$). However, the average sPSC time courses of the two cells types were different (inset in Fig. 3*D*). The layer II neurone had a rise time of 3.1 ± 4.2 ms and a half-width of 15.4 ± 16.2 ms (inset, black line). The CA1 neurone had an average rise time of 11.5 ± 9.8 and half-width of 50.4 ± 61.8 ms (grey line).

In seven such sequential recordings, there was a significant difference in the average sPSC frequency, which was 30 ± 13 Hz in layer II neurones and 4 ± 4 Hz in CA1 pyramids ($P_{pt} < 0.001$). There was no significant difference for the average sPSC amplitudes, which for neocortical and CA1 cells were 6.4 ± 2.3 and 6.1 ± 1.5 pA, respectively ($P_{pt} = 0.8$). Averaged across the cells, sPSCs in layer II cortical cells had significantly faster rise times than CA1 neurones (5.4 ± 0.9 *versus* 10.6 ± 4.9 ms; $P_{pt} = 0.017$). In addition, sPSCs in layer II had shorter half-widths (10.9 ± 2.9 *versus* 18.5 ± 9.5 ms; $P_{pt} = 0.03$). These differences may be due to a poorer space-clamp in CA1 cells, as in this paired data they had a lower R_i (250 ± 220 MΩ) than layer II neurones (340 ± 90 MΩ). Alternatively, the differences in time course may be caused by differences in synaptic locations on the dendrites or in receptor kinetics. From this set of experiments we concluded that the high rate of sPSCs was a genuine feature of synapses in layer II.

To determine whether the synaptic currents recorded in layer II were primarily the result of spontaneous action potentials, 1 μM TTX was added to the ACSF to block voltage-dependent Na^+ channels (Fig. 4). In this example, the average frequency changed from 20 ± 1 to 18 ± 1 Hz, and the average f_1 was reduced from 65 ± 83 to 49 ± 65 Hz. However, there was no significant shift in the cPDFs of either f_1 ($P_{KS} = 0.15$) or amplitudes (6.8 ± 5.2 before and 7.0 ± 5.4 pA after TTX; $P_{KS} = 0.20$).

Across 18 experiments, 1 μM TTX failed to produce any significant change in either the average PSC frequency

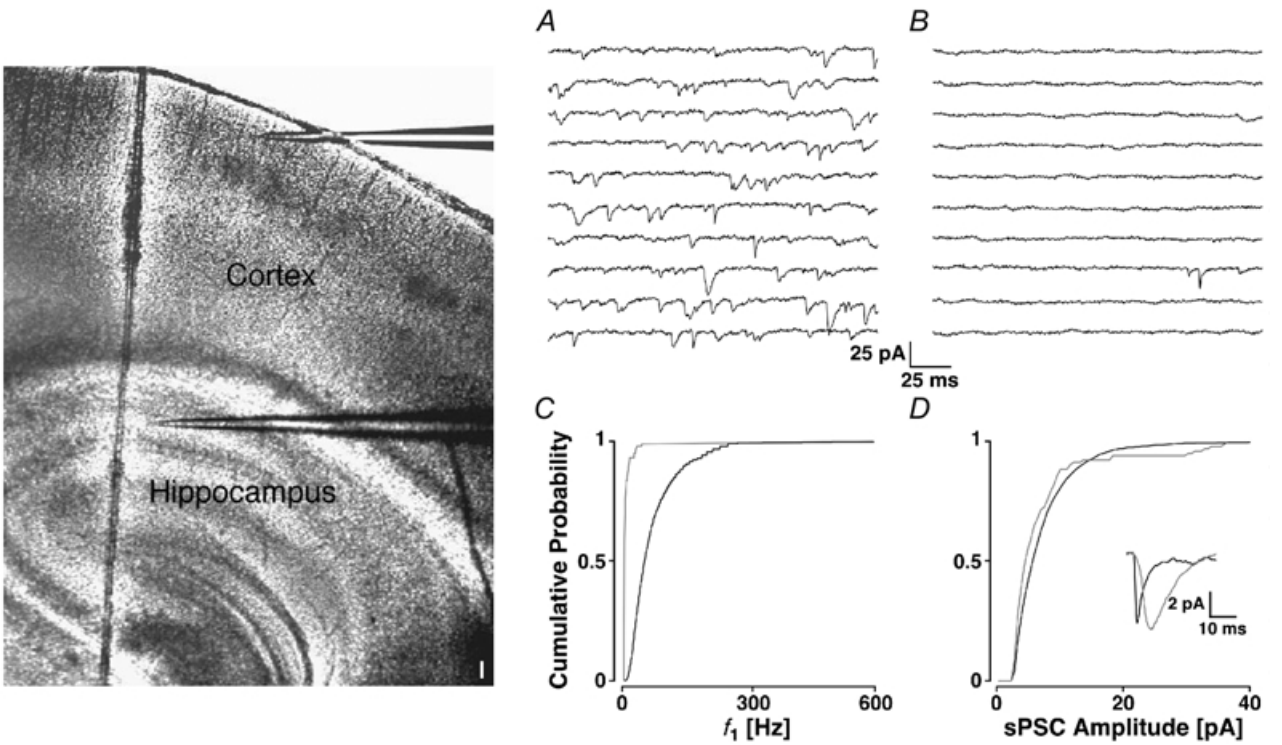

Figure 3. sPSCs in neocortex and hippocampus

Two positions are illustrated by the placement of the recording electrodes in the photomontage of two IR-DIC images of a parasagittal slice. Barrels can be identified in somatosensory cortex (darker spots) and the cell layers in hippocampus (scale bar 100 μm). The sequences of the recording from a pyramidal cell in layer II of somatosensory cortex (*A*) and CA1 of hippocampus (*B*). The cPDFs of f_1 (*C*) and amplitudes (*D*) for the neocortical (black line) and hippocampal neurone (grey line). The average sPSC time courses are illustrated in the inset.

(31 ± 23 Hz before and 28 ± 24 Hz after the addition of TTX, $P_{pt} = 0.20$), or amplitude (11 ± 4 pA and 10 ± 3 pA, respectively; see also Fig. 5*G* and *H* for the relative changes). The average time course was slightly briefer, but statistically not changed (inset in Fig. 4*D*; $P_{pt} = 0.07$). In Fig. 4*E* and *F*, the average frequencies and amplitudes, respectively, in TTX (mPSC) are plotted against the value in control conditions (sPSC). The black lines represent the linear fits of the data points, the slopes of which were 0.99 and 0.97, respectively. Both fitted lines were not different from the line of equality ($P > 0.05$; analysis of covariance with $n = 18$). These results suggest that the vast majority of sPSCs are the result of a process that is independent of action potentials and, therefore, likely to be restricted to the synaptic terminal. These currents are subsequently called miniature PSCs (mPSCs).

Most of the mPSCs are excitatory

We investigated the synaptic origin of the mPSCs by applying the $GABA_A$ receptor blocker bicuculline methiodide (10 μM). In the example presented in Fig. 5*A–D* of a recording from a layer II pyramidal cell, bicuculline had no effect on the average mPSC frequency, which was 91 ± 5 before and 93 ± 5 Hz after the addition of the $GABA_A$ blocker. This is also illustrated in the cPDFs of f_1 (Fig. 4*C*), in which the mean of f_1 was 140 ± 103 Hz before and 146 ± 113 Hz after the addition of bicuculline ($P_{KS} = 0.62$). This drug also failed to significantly shift the amplitude distribution (Fig. 4*D*; mean 7.1 ± 5 *versus* 6.6 ± 4.0 pA, $P_{KS} = 0.35$). The results from 10 experiments indicated that this treatment failed to produce any significant difference in mPSC frequency or amplitude (98.1 ± 2.0 % and 97.0 ± 9.7 % of control; $P_{pt} > 0.05$; see Fig. 5*G* and *H*).

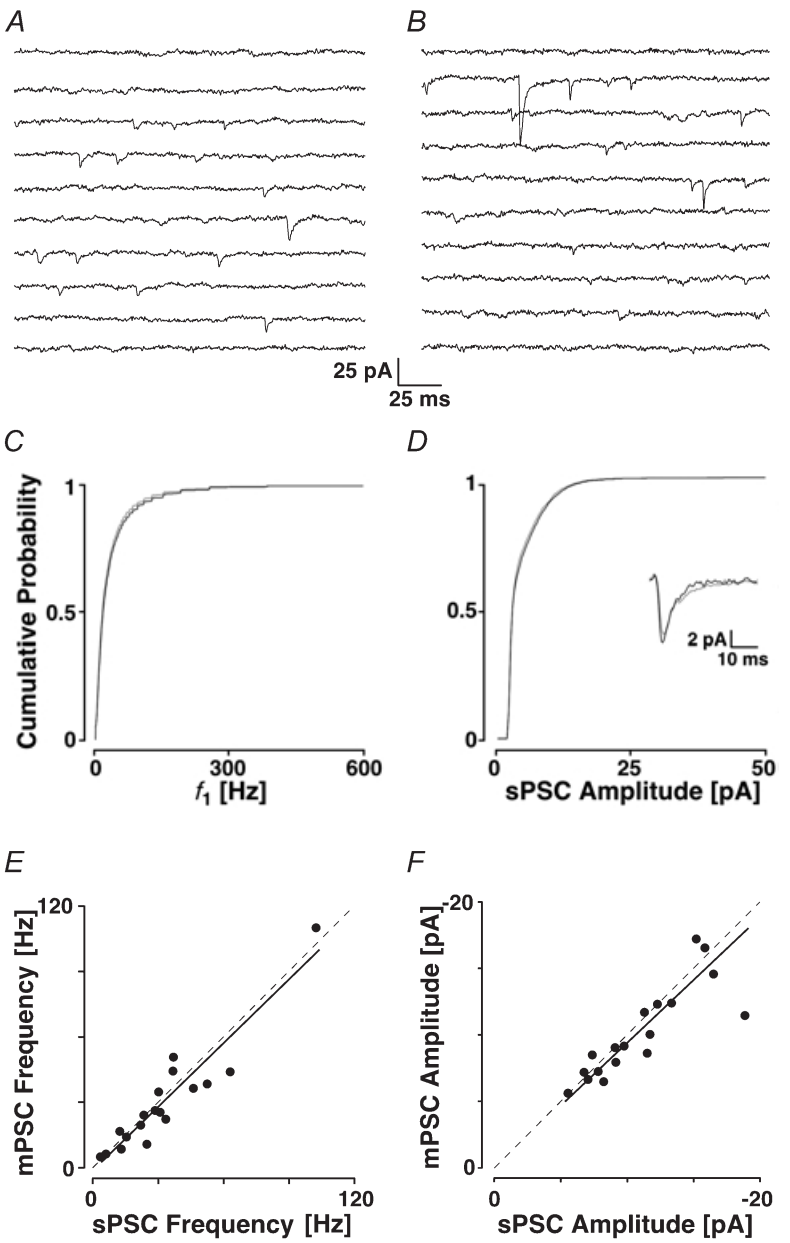

Figure 4. Block of sodium channels does not reduce mEPSC frequency

In *A* a recording epoch is shown before and in *B* after the addition of 1 μM TTX. The cPDFs of f_1 (*C*) and amplitudes (*D*) before (black line) and after the addition of TTX (grey line). In both *C* and *D*, the cPDFs are not different from each other. The average sPSC time courses are shown in the inset. *E* and *F*, the average mPSC frequencies and amplitudes (in TTX) are plotted against those in control solution (for $n = 18$). Note that the points in both graphs cluster around the dashed line, which represents equality. The continuous line represents the linear fit to the data.

The average mPSC time course remained unchanged. These results suggest that the mPSCs are primarily of excitatory synaptic origin and they are subsequently called mEPSCs.

The glutamatergic origin of the mEPSCs was confirmed with a specific and potent AMPA receptor antagonist, NBQX (10 μM), which produced a complete block of all mEPSCs within 5 min of its addition to the ACSF (Fig. 5*E* and *F*). A similar result was obtained with 1 mM kynurenic acid, a broadband blocker of glutamatergic transmission (see also summary in Fig. 5*G* and *H*), which showed an incomplete block at the concentration used. Even in experiments with the highest mEPSC frequencies, blocking AMPA receptors did not reveal any change in R_{in}, nor any systematic change in holding current, indicating that the rate of mEPSCs was insufficient to cause a tonic AMPA current.

Excitability changes

We checked if changes in excitability caused the high rate of mEPSCs either by an increase in extracellular K^+ from damaged cells, increased glutamate availability or spontaneous gating of VDCCs.

We assayed the first question with solutions of reduced K^+ composition. Using the Goldmann-Hodgkin-Katz equation, lowering extracellular K^+ either to 1 or 0.1 mM should result in a hyperpolarisation of 4 or 6 mV, respectively. Experimentally, the reduction of extracellular K^+ was accompanied by a shift in holding current between 10 and 60 pA, confirming that this manipulation caused a hyperpolarisation. In nine experiments, lowering K^+ concentration resulted in no significant change in either frequency or amplitude (see Fig. 5*G* and *H*, low excitability solution (LES)).

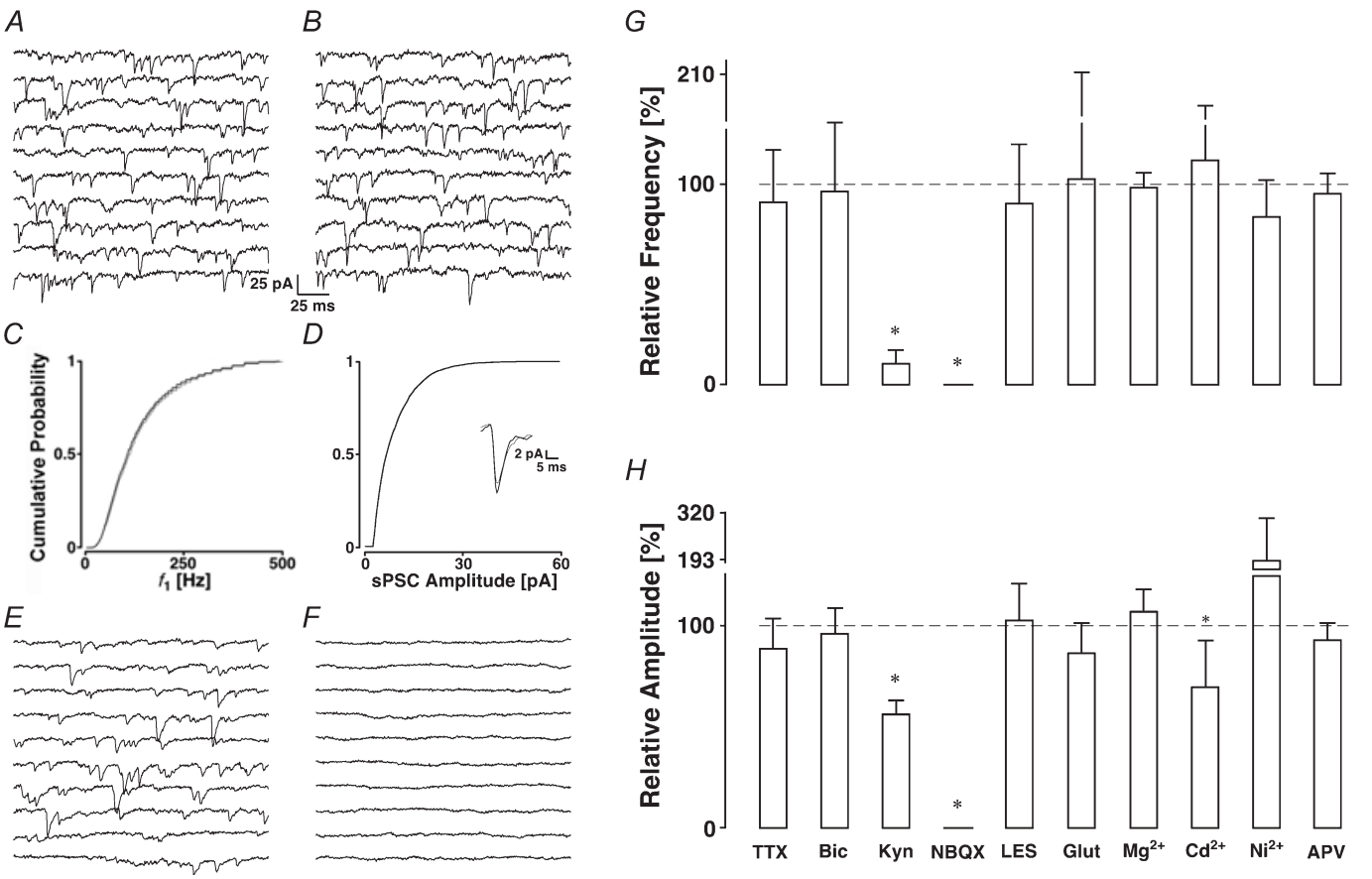

Figure 5. Pharmacological profile of mEPSCs

A, control recording epoch and *B*, after the addition of bicuculline. The cPDFs of f_1 (*C*) and amplitudes (*D*) before (black line) and after the block of inhibition (grey line) with the average time courses shown in the inset. mEPSCs are mediated by AMPA receptors; *E*, recording epoch in control ACSF and *F*, after the addition of 10 μM NBQX. Pharmacological measures to reduce the frequency (*G*) and amplitude (*H*) of mEPSCs show that only AMPA receptor blockade has an effect on mPSC frequency. Data are pooled after normalising to control condition. Asterisks indicate significant changes. The abbreviations indicate ACSF to which tetrodotoxin (TTX, $n = 18$), bicuculline (Bic, $n = 10$), kynurenic acid (Kyn, $n = 6$), NBQX ($n = 3$), glutamine (Glut, $n = 5$), Mg^{2+} ($n = 5$), Cd^{2+} ($n = 7$), Ni^{2+} ($n = 5$) or APV ($n = 6$) was added. LES indicates low excitability solution ($n = 9$).

Glutamate is produced in neurones from glutamine taken up from glia. Hence, we thought that glutamate biosynthesis might play a role. We added 1 mM glutamine, as the precursor of glutamate, to the ACSF (Larkman *et al.* 1992). This changed neither rate nor amplitude of mEPSCs (see Fig. 5*G* and *H*).

We tested the hypothesis that spontaneous gating of VDCCs triggered mEPSCs both by lowering extracellular Ca^{2+} and by blocking VDCCs with divalent cations. Lowering Ca^{2+} to 0.5 mM while increasing Mg^{2+} to 6 mM did not produce any significant changes in mEPSC frequency or amplitude. Also block of VDCCs with either 100 μM Cd^{2+} or 100 μM Ni^{2+} did not cause changes, except that block with Cd^{2+} produced a decrease in mEPSC amplitude to 77 ± 20 % of the control value, which was significant ($P_{pt} = 0.02$).

There is evidence for the presence of presynaptic NMDA receptors (Smirnova *et al.* 1993; DeBiasi *et al.* 1996) and NMDA receptors with *I–V* relationships shifted to more negative potentials (Fleidervish *et al.* 1998), which could therefore be active under resting conditions. Spontaneous gating of these receptors would allow an influx of Ca^{2+}. We therefore tested if the addition of 50 μM D,L-APV had an effect on mEPSC characteristics. Again, we found no significant changes (see Fig. 5*G* and *H*).

This set of experiments suggests that the high rate of mEPSCs is not caused by external factors but might reflect a general property of the terminals onto layer II cells.

Kinetic properties of mEPSCs

In order to get insight into the kinetics of the mEPSCs, data sets were scanned for the fastest mEPSCs in both rise time and half-width. We concentrated on the fastest 10 % of

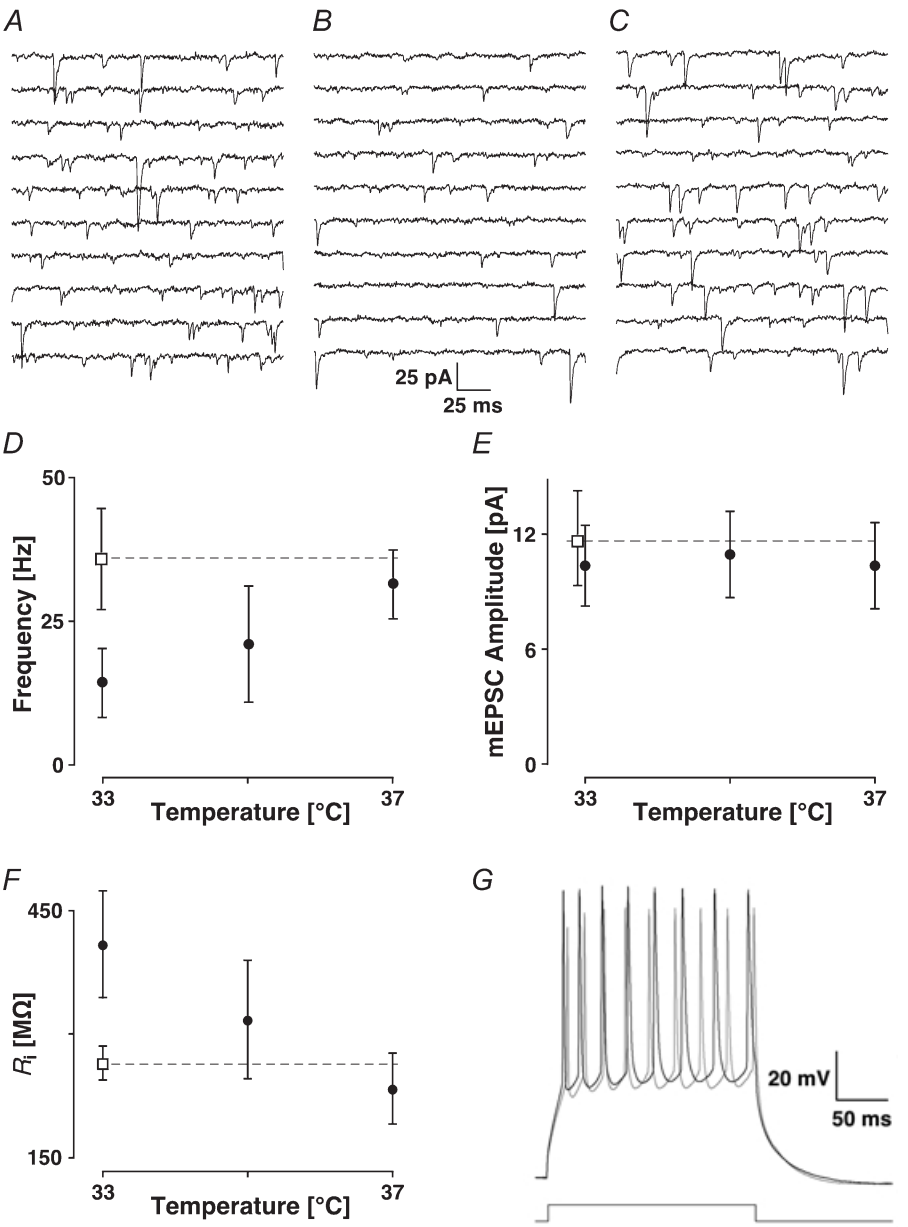

Figure 6. Temperature sensitivity

Recording sequences are shown in *A* at 33 °C with the IR light on, in *B* at the same temperature but with the microscope lamp turned off and in *C* at 37 °C without light. The average mEPSC frequencies (*D*) and amplitudes (*E*) are plotted as a function of recording temperature without light (●) and with light on (□). The dashed line helps to extrapolate the higher frequency to the higher temperature. Note that the mEPSC amplitude has little dependence on temperature. In *F*, the input resistance is plotted as a function of temperature with the same symbol code as in the two previous figures. *G*, bursts of action potentials caused by current injection of 0.3 nA are illustrated at 33 °C without (black line) and with the light switched on (grey line).

mEPSCs. Since the conjunction of both rise time and half-width was required, the identified set of mEPSCs was smaller than the 10 % of the originally reported number of events.

In 10 experiments, where large sets of mEPSCs were recovered (on average 8649 ± 2482), some 400 ± 76 mEPSCs were identified. This represented 7.6 ± 4.3 % of the total number of observations. The 10–90 % rise time of these mEPSCs was 288 ± 86 μs (range 167–441 μs) and the half-width was 1073 ± 532 μs (range 330–2157 μs). The amplitudes of these fastest events had a magnitude of 5.9 ± 1.1 pA and a CV of 0.44 ± 0.14.

Temperature sensitivity of mEPSCs

During the course of the experiments, we observed a large variation in the frequency of mEPSCs, depending on whether the microscope lamp was turned on or not. Since the condenser focuses IR light into a small volume of the slice, the resulting heat might have been the cause for the variation in frequency. We therefore investigated the temperature sensitivity of mEPSCs.

Figure 6*A–C* shows recording sequences from a pyramidal neurone with ACSF heated to 33 °C and the IR light turned on (*A*), with the light turned off (*B*), and turned off but heated to 37 °C (*C*). In *A*, an average mEPSC frequency of 38 ± 2 Hz and amplitude of 12.6 ± 10.0 pA were found. In *B*, the frequency and amplitude were reduced to 15 ± 1 Hz and 12.0 ± 9.9 pA. When the temperature was subsequently increased to 37 °C, the frequency and amplitude were 36 ± 2 Hz and 12.6 ± 8.8 pA, close to the values obtained at 33 °C but with the infrared light on. Only the changes in frequency were significant.

The data from five experiments with similar rates of mEPSCs are plotted as a function of temperature in Fig. 6*D* and *E* for the frequencies and amplitudes, respectively. Switching the lamp off (filled circle) or defocusing the condenser produced a significant reduction in the mEPSC frequency to 39 ± 7 % of the frequency recorded with the lamp switched on ($P_{pt} < 0.001$; open square), but did not affect the amplitude (90 ± 18 % of control; $P_{pt} = 0.29$). When the ACSF was heated to 37 °C, the average mEPSC frequency was not significantly different from when the ACSF was heated to 33 °C, but the light switched on.

Since mEPSCs are unlikely to be well voltage-clamped, a temperature-induced change in passive and/or active membrane properties could result in a change in the rate of mEPSCs. We measured the input resistance of layer II pyramidal cells. Increasing the temperature from 33 to 37 °C led to a linear decrease in R_{in} (Fig. 6*F*). In the same experiment, a current injection of 0.3 nA over 200 ms resulted in a burst of action potentials, which showed a higher frequency with smaller amplitudes with the light on than off (Fig. 6*G*). We therefore considered it unlikely that changes in active/passive properties are responsible for the temperature sensitivity. These data indicate the importance of specifying the recording conditions with the IR-DIC method.

Table 1. Cell-type specific properties

Cell type	*N*	f_0 (Hz)	Mean (pA)	R_{in} (MΩ)	R_s (MΩ)
Pyramidal	29	45 ± 4	9.1 ± 2.2	245 ± 170	11.5 ± 2.7
Multipolar	10	41 ± 7	9.3 ± 1.7	225 ± 135	12.9 ± 3.0
Bipolar	23	15 ± 1	8.3 ± 3.5	270 ± 195	15.0 ± 2.7

f_0 indicates the average frequency, R_{in} corresponds to the input resistance and R_s to the series resistance

To gain insight into the temperature dependence of mEPSC release, a series of experiments was performed in which the rate of mEPSCs was measured at different temperatures between 33 and 37 °C. The natural logarithm of the relative change in frequency was plotted as a function of one over temperature and the slope estimated which corresponds to the logarithm of Q_{10} (Johnson *et al.* 1954, data not shown). This resulted in a value of 8.9 ± 0.9 over the range specified ($r = 0.85$; $P_r < 0.0001$; $n = 16$).

Cell-type specificity

We noticed differences in the rate of mEPSCs from recording to recording and investigated whether there were differences in mEPSC frequency between the different cell types. Table 1 shows the pooled data from 62 cells, which were histologically identified. There is a striking difference in the mEPSC frequency between pyramidal/multipolar cells and the bipolar cell, with the latter showing a much lower frequency. The average frequency of the bipolar cells was about a third of that in pyramidal or multipolar cells (15 ± 1 *versus* 45 ± 4 and 41 ± 7, respectively; $P_t < 0.001$). There were no differences in frequency between pyramidal and multipolar cells ($P_t = 0.64$). Between the three cell types, there were no differences for other parameters measured, such as mEPSC amplitude, time course, R_s and R_{in}.

DISCUSSION

In this paper, we have characterised mEPSCs in layer II pyramidal cells of young rats. The major findings are that the rate of mEPSCs is high compared to other preparations, that the rate is highly temperature sensitive and that there are cell-specific differences.

mEPSC characteristics

The finding that the average mEPSC frequencies were as high as 100 Hz came as a surprise. Based on recordings in CA1 of the hippocampus, we were able to rule out that this observation was caused by a slicing artefact (hypoxic insult), slice superfusion or tissue viability. The rate found in CA1 pyramidal cells is consistent with earlier reports (Manabe *et al.* 1992). If hypoxia were a factor, we would

have expected a sharp increase in mEPSC frequency in CA1 but a decrease in neocortical cells (Fujiwara *et al.* 1987; Jiang & Haddad, 1992).

Blocking action potentials with TTX did not result in a significant reduction in the frequency of mEPSCs. Since the neurones receive a large fraction of input from neurones nearby (Gruner *et al.* 1974), the lack of effect of TTX on mEPSC frequency implies that most presynaptic neurones are silent, at least in the slice preparation. Indeed, we have never observed spontaneous action potentials either in cell-attached (before break-in) or in whole-cell mode. Similar observations have been reported in neocortical tissue by others (for example Hutcheon *et al.* 1996; but also see Mao *et al.* 2001). Our observations are in line with more recent reports using *in vivo* whole-cell recordings, which show that the rate of spontaneous firing in somatosensory cortex is low (Moore & Nelson, 1998; Zhu & Connors, 1999; Brecht & Sakmann, 2002) and does not result from changes in intracellular electrolyte caused by the recording electrode (Margrie *et al.* 2002). Such findings are, however, in contrast to extracellular unit recordings, in which significantly higher spontaneous rates have been reported (Simons, 1978; Huang *et al.* 1998). *In vivo* recordings also show that neurones in intact tissue can be in two different states: in a hyperpolarised or a depolarised state (Steriade *et al.* 2001; Brecht & Sakmann, 2002). It might be that due to the slicing procedure, neurones in slices tend to be in the hyperpolarised state and do not show spontaneous firing. Given the evidence from *in vitro* and *in vivo* whole-cell recordings, it is conceivable that TTX does not show a significant reduction of mEPSC frequency.

We provide evidence that there is very little contribution by GABAergic synapses to the frequency of mPSCs, since under our recording conditions, with the chloride currents reversed, we should have been able to detect mIPSCs. In our preparation, the rate of mIPSCs was only a few hertz compared to about 40 Hz for mEPSCs (resolution). This differs slightly from Salin & Prince (1996), who reported a preponderance of mIPSCs in layer III (2–16 Hz). The difference is likely explained by the age difference. In our experiments, inhibitory synapses are developing, but are fully matured at 30–45 days (Luhmann & Prince, 1991), the age of the animals studied by Salin & Prince (1996).

mEPSPs in rats neocortex have previously been described (Hardingham & Larkman, 1998). These authors found mEPSP rates of up to 14.6 Hz at 36 °C in animals slightly older than the ones in this study. We do not think that the difference in frequency is due to an age difference since we saw similar rates in older animals (around 24 days). Current-clamp recording will have resulted in a systematic underestimation of miniature rates. However, a bigger difference might have been caused by the localisation of the cells recorded from since we concentrated largely on upper layer II cells whereas Hardingham & Larkman (1998) recorded in layer II–III.

The parameters of the fastest mEPSC time courses are consistent with AMPA receptor-mediated currents and this was confirmed pharmacologically. However, the time courses were slightly longer than those reported in other studies (Finkel & Redman, 1983; Silver *et al.* 1992; Jonas *et al.* 1993). We think that this difference is largely due to insufficient space-clamp since excitatory synapses are not on somata of layer II pyramidal cells (Larkman, 1991) and because we did not routinely compensate series resistance or electrode and whole-cell capacitance.

We observed changes in neither R_{in} nor holding current when AMPA receptors were blocked. This contrasts with mIPSCs in hippocampus (Otis *et al.* 1991) where a tonic GABAergic current can be measured. As AMPA conductances are only activated for 2–3 ms, a tonic current would therefore require an average frequency of > 300 Hz.

The classic concept of mEPSCs suggests that they are the result of vesicular release from presynaptic nerve terminals (Katz & Miledi, 1963). However, there is evidence that in addition glia, and in particular astrocytes (Parpura *et al.* 1994; Parri *et al.* 2001), as well as dendrites of other pyramidal cells (Zilberter, 2000) are capable of releasing glutamate. We, therefore, are unable to directly confirm that the mEPSCs in this study originated from nerve terminals. Since release of glutamate from astrocytes requires the activation of NMDA receptors, and since blocking these receptors did not change the frequency of mEPSCs, we think that astrocytes are an unlikely source of mEPSCs in our preparation.

Neither lowering extracellular K^+ to change excitability, nor changing glutamate availability, nor blocking VDCCs caused significant changes in mEPSC frequency. Together, these results suggest that the high rate of mEPSCs is a basic feature of terminals in this cell layer.

Temperature had a very pronounced effect on the rate of mEPSCs which could be mimicked by turning on the IR light source. With the optics used on our set-up, we extrapolated that the temperature in the focal volume was increased by about 4 °C. The increase in temperature was accompanied by a decrease in R_{in} of the cell. The smaller R_{in} at the higher temperature would lead to a poorer space-clamp with fewer distal synapses having current amplitudes above the recording noise. An increased temperature might speed up the kinetics of the AMPA conductance. There is the possibility that the concomitant decrease in R_{in} might have masked the faster kinetics. However, we could not detect faster AMPA current kinetics at higher temperatures. The change in mEPSC rate is, therefore,

unlikely to have been caused by changes in passive properties of the cell, since lowering R_{in} should have reduced the amplitudes of mEPSCs under insufficient voltage-clamp conditions.

We estimated that the temperature coefficient of the frequency change, Q_{10} (33–37 °C), was 8.9 ± 0.9. This value is in accordance with the study of Barrett *et al.* (1978), who found a value of close to 10, but is in contrast to other studies at the neuromuscular junction, which typically reported a value of 3–4. The high Q_{10} indicates that an appreciable activation energy (17.3 ± 1.6 kJ) needs to be overcome for vesicles to be released, which is consistent with significant energy consumption during the docking process.

Cell type-specific differences

The use of IR-DIC optics enabled us to select visually the cell types for recording and subsequent histological confirmation. mEPSCs occurred three times more frequently in pyramidal and multipolar cells than in bipolar cells. Possible explanations for this could be a lower synaptic density or a reduced dendritic surface area. In mouse somatosensory cortex, bipolar cells have an innervation density, which is double that of multipolar cells. Also the proportion of synapses formed by thalamocortical axon terminals onto bipolar cells is six times greater than that formed on multipolar cells (White & Rock, 1981). Overall, the density of synapses on bipolar cells from sources other than the thalamus is 83 % (White & Rock, 1981). Therefore, it is unlikely that a lower synaptic density is the cause for a reduced frequency. At this stage, we do not know whether the lower frequency is the result of a smaller dendritic area or simply reflects an intrinsic difference in the properties of the presynaptic terminals (target-cell specificity).

The role of a high rate of mEPSCs for development and physiology is largely unknown. In development, spontaneous activity is required for synapse formation and stabilisation. At least in cultures, spontaneous activation of AMPA receptors serves to maintain spines (McKinney *et al.* 1999). Physiologically, mEPSCs might modulate membrane properties by continually changing the membrane potential and thereby affecting activation/inactivation properties of voltage-dependent channels and tuning postsynaptic membranes. Such a property could be used to increase the signal-to-noise ratio of weak synaptic signals (Stacey & Durand, 2001). The very much smaller rate of mEPSCs as seen in bipolar cells might allow interneurones to exert their crucial role in synchronising networks (Traub *et al.* 1996).

In the accompanying paper (Simkus & Stricker, 2002) we investigate whether intracellular calcium when released from stores might cause spontaneous release.

REFERENCES

Barrett, E. F., Barrett, J. N., Botz, D., Chang, D. B. & Mahaffey, D. (1978). Temperature-sensitive aspects of evoked and spontaneous transmitter release at the frog neuromuscular junction. *Journal of Physiology* **279**, 253–273.

Brecht, M. & Sakmann, B. (2002). Dynamic representation of whisker deflection by postsynaptic potentials in morphologically reconstructed spiny stellate and pyramidal cells in the barrels and septa of layer 4 in rat somatosensory cortex. *Journal of Physiology* **543**, 49–70.

Clements, J. D. & Bekkers, J. M. (1997). Detection of spontaneous synaptic events with an optimally scaled template. *Biophysical Journal* **73**, 220–229.

Debiasi, S., Minelli, A., Melone, M. & Conti, F. (1996). Presynaptic NMDA receptors in the neocortex are both auto- and heteroreceptors. *NeuroReport* **7**, 2773–2776.

Finkel, A. S. & Redman, S. J. (1983). The synaptic current evoked in cat spinal motoneurones by impulses in single group Ia axons. *Journal of Physiology* **342**, 615–632.

Fleidervish, I. A., Binshtok, A. M. & Gutnick, M. J. (1998). Functionally distinct NMDA receptors mediate horizontal connectivity within layer 4 of mouse barrel cortex. *Neuron* **21**, 1055–1065.

Fujiwara, N., Higashi, H., Shimoji, K. & Yoshimura, M. (1987). Effects of hypoxia on rat hippocampal neurones *in vitro*. *Journal of Physiology* **384**, 131–151.

Gilbert, C. D. (1976). Laminar differences in receptive field properties of cells in cat primary visual cortex. *Journal of Physiology* **268**, 391–421.

Gruner, J. E., Hirsch, J. C. & Sotelo, C. (1974). Ultrastructural features of the isolated suprasylvian gyrus in the cat. *Journal of Comparative Neurology* **154**, 1–24.

Hardingham, N. R. & Larkman, A. U. (1998). The reliability of excitatory synaptic transmission in slices of rat visual cortex *in vitro* is temperature dependent. *Journal of Physiology* **507**, 249–256.

Horikawa, K. & Armstrong, W. E. (1988). A versatile means of intracellular labeling: Injection of biocytin and its detection with avidin conjugates. *Journal of Neuroscience Methods* **25**, 1–11.

Huang, W., Armstrong-James, M., Rema, V., Diamond, M. E. & Ebner, F. F. (1998). Contribution of supragranular layers to sensory processing and plasticity in adult rat barrel cortex. *Journal of Neurophysiology* **80**, 3261–3271.

Hutcheon, B., Miura, R. M. & Puil, E. (1996). Subthreshold membrane resonance in neocortical neurons. *Journal of Neurophysiology* **76**, 683–697.

Jiang, C. & Haddad, G. G. (1992). Differential responses of neocortical neurons to glucose and/or O_2 deprivation in human and rat. *Journal of Neurophysiology* **68**, 2165–2173.

Johnson, F. H., Eyring, H. & Polissar, M. J. (1954). *The Kinetic Basis of Molecular Biology*. John Wiley & Sons, Ltd, New York, London.

Jonas, P., Major, G. & Sakmann, B. (1993). Quantal components of unitary EPSCs at the mossy fibre synapse on CA3 pyramidal cells of rat hippocampus. *Journal of Physiology* **472**, 615–663.

Katz, B. & Miledi, R. (1963). A study of spontaneous miniature potentials in spinal motoneurons. *Journal of Physiology* **168**, 389–422.

Kawaguchi, Y., Wilson, C. J. & Emson, P. C. (1989). Intracellular recording of identified neostriatal patch and matrix spiny cells in a slice preparation preserving cortical inputs. *Journal of Neurophysiology* **62**, 1052–1068.

Keller, A. (1995). Synaptic organization of the barrel cortex. In *The Barrel Cortex of Rodents*, ed. Jones, E. G. & Diamond, I. T., pp. 221–262. Plenum Press, New York and London.

Larkman, A. U. (1991). Dendritic morphology of pyramidal neurones of the visual cortex of the rat: III. Spine distributions. *Journal of Comparative Neurology* **306**, 332–343.

Larkman, A. U., Hannay, T., Stratford, K. J. & Jack, J. J. B. (1992). Presynaptic release probability influences the locus of long-term potentiation. *Nature* **360**, 70–73.

Luhmann, H. J. & Prince, D. A. (1991). Postnatal maturation of the GABAergic system in rat neocortex. *Journal of Neurophysiology* **65**, 247–263.

McKinney, R. A., Capogna, M., Dürr, R., Gähwiler, B. H. & Thompson, S. M. (1999). Miniature synaptic events maintain dendritic spines via AMPA receptor activation. *Nature Neuroscience* **2**, 44–49.

Manabe, T., Renner, P. & Nicoll, R. A. (1992). Postsynaptic contribution to long-term potentiation revealed by the analysis of miniature synaptic currents. *Nature* **355**, 50–55.

Mao, B.-Q., Hamzei-Sichani, F., Aronov, D., Froemke, R. C. & Yuste, R. (2001). Dynamics of spontaneous activity in neocortical slices. *Neuron* **32**, 883–898.

Margrie, T. W., Brecht, M. & Sakmann, B. (2002). In vivo low-resistance, whole-cell recordings from neurons in the anaesthetized and awake mammalian brain. *Pflügers Archiv* **444**, 491–498.

Moore, C. I. & Nelson, S. B. (1998). Spatio-temporal subthreshold receptive fields in the vibrissa representation of rat primary somatosensory cortex. *Journal of Neurophysiology* **80**, 2882–2892.

Otis, T. S., Staley, K. J. & Mody, I. (1991). Perpetual inhibitory activity in mammalian brain slices generated by spontaneous GABA release. *Brain Research* **545**, 142–150.

Paré, D., Lebel, E. & Lang, E. J. (1997). Differential impact of miniature synaptic potentials on the soma and dendrites of pyramidal neurons in vivo. *Journal of Neurophysiology* **78**, 1735–1739.

Parpura, V., Basarsky, T. A., Liu, F., Jeftinija, K., Jeftinija, S. & Haydon, P. G. (1994). Glutamate-mediated astrocyte-neuron signalling. *Nature* **369**, 744–747.

Parri, H. R., Gould, T. M. & Crunelli, V. (2001). Spontaneous astrocytic Ca^{2+} oscillations in situ drive NMDAR-mediated neuronal excitation. *Nature Neuroscience* **4**, 803–812.

Salin, P. A. & Prince, D. A. (1996). Spontaneous $GABA_A$ receptor-mediated inhibitory currents in adult rat somatosensory cortex. *Journal of Neurophysiology* **75**, 1573–1588.

Silver, R. A., Traynelis, S. F. & Cull-Candy, S. G. (1992). Rapid-time-course miniature and evoked excitatory currents at cerebellar synapses in situ. *Nature* **355**, 163–166.

Simkus, C. R. L. & Stricker, C. (2002). The contribution of intracellular calcium stores to mEPSCs recorded in layer II neurones of rat barrel cortex. *Journal of Physiology* **545**, 521–535.

Simons, D. J. (1978). Response properties of vibrissa units in rat SI somatosensory neocortex. *Journal of Neurophysiology* **41**, 798–820.

Smirnova, T., Stinnakre, J. & Mallet, J. (1993). Characterization of a presynaptic glutamate receptor. *Science* **262**, 430–433.

Stacey, W. C. & Durand, D. M. (2001). Synaptic noise improves detection of subthreshold signals in hippocampal CA1 neurons. *Journal of Neurophysiology* **86**, 1104–1112.

Steriade, M., Timofeev, I. & Grenier, F. (2001). Natural waking and sleep states: A view from inside neocortical neurons. *Journal of Neurophysiology* **85**, 1969–1985.

Stuart, G. J., Dodt, H.-U. & Sakmann, B. (1993). Patch clamp recordings from the soma and dendrites of neurons in brain slices using infrared video microscopy. *Pflügers Archiv* **423**, 511–518.

Traub, R. D., Whittington, M. A., Stanford, I. M. & Jefferys, J. G. R. (1996). A mechanism for generation of long-range synchronous fast oscillations in the cortex. *Nature* **383**, 621–624.

White, E. L. & Rock, M. P. (1981). A comparison of thalamocortical and other synaptic inputs to dendrites of two non-spiny neurons in a single barrel of mouse SmI cortex. *Journal of Comparative Neurology* **195**, 265–277.

Zhu, J. J. & Connors, B. W. (1999). Intrinsic firing patterns and whisker-evoked synaptic responses of neurons in the rat barrel cortex. *Journal of Neurophysiology* **81**, 1171–1183.

Zilberter, Y. (2000). Dendritic release of glutamate suppresses synaptic inhibition of pyramidal neurons in rat neocortex. *Journal of Physiology* **528**, 489–496.

Acknowledgements

We thank Drs Anna Cowan, Urs Gerber and Steve Redman for their comments on earlier drafts of this manuscript. This work was supported by grants from the Swiss National Science Foundation (5002-42787 and 5002-057809).